DOI: https://doi.org/10.68732/ea5b4bf967eda626

ISBN: 978-9989-2053-6-1

Plastic swelling and hardening mechanisms of in-situ heated Callovo-Oxfordian claystone

J. Ren & P. Braun & S. Ghabezloo
École nationale des ponts et chaussées, Champs-sur-Marne, France
philipp.braun@enpc.fr
0000-0003-3207-5018

C. Plua & M. Vu
Andra, Châtenay-Malabry, France

Abstract

Callovo-Oxfordian (COx) claystone is the candidate host rock for the future French deep geological repository for radioactive waste, designed to experience thermal loads of up to 90°C during operation. In this context, this study characterizes cores extracted after an in-situ heating test where the maximum temperature reached 95°C. A multistep isotropic test was performed on a sample resaturated close to the in-situ stress state. Drained and repeated mechanical unloading-reloading cycles were carried out. Reversible elastic strain and irreversible plastic strain were decomposed from specially designed loading steps to characterize the evolution of plastic yield mechanisms. Results indicate that the sample exhibited plastic swelling during the unloading paths, when the effective mean stress decreased below 8 MPa. The unloading also seemed to have reduced the compression yield limit, since during subsequent reloading, we observed plastic compression at stress levels below the initial state. Furthermore, unloading after loading to high confining pressure revealed that the swelling yield limit increased, exceeding the initial stress level, thereby demonstrating a hardening effect. These observations could be represented by a swelling yield limit at a low effective mean stress, which is strongly coupled with the compression yield limit during the hardening process. The observed swelling during mechanical unloading could be relevant for in-situ stress paths involving decreasing mean effective stress, namely tunnel excavation, fracture self-sealing, thermal pressurization and retrieval of laboratory specimens.

Keywords

Callovo-Oxfordian claystone, In-situ heating, Elasto-plastic behaviour, Plastic swelling, Stress release.

1 Introduction

Callovo-Oxfordian (COx) claystone is the candidate host rock for the future French deep geological repository for radioactive waste, located in the north-east of France. In the design of this repository, COx claystone is expected to experience thermal loads of up to 90 °C during operation. To better understand the response of COx under the complex thermo-hydro-mechanical (THM) loading, various in-situ and laboratory tests have been conducted across different scales (Belmokhtar et al. 2017; Zhang et al. 2019; Braun et al. 2021; Bumbieler et al. 2021; Plúa et al. 2024). It should be noted that before laboratory investigations, the material undergoes complex sequences such as excavation and core extraction, which could induce moisture loss and stress release.

The influence of desaturation on the mechanical performance of clayey rocks has been studied. Ewy (2015) demonstrated that moisture loss during the deconfinement can lead to performance degradation and structural damage. Conil et al. (2018) further emphasized the importance of core extraction and conditioning procedures, leading to the development of special storage cells designed to minimize the effects of desaturation and stress release. Nevertheless, the specific impact of mechanical unloading on the plastic mechanisms of the material is not yet fully understood. Research on similar clay-rich formations, such as the Opalinus claystone, has suggested that the excavation-induced response is not purely linear-elastic (Corkum and Martin 2007). Therefore, investigating the unloading process of COx claystone is important to evaluate the impact of stress release history on its subsequent mechanical properties.

To this end, the present study utilizes a core extracted after an in-situ heating experiment conducted by Andra in the Meuse/Haute-Marne Underground Research Laboratory (MHM URL). One specimen was resaturated and subjected to a series of multi-step isotropic unloading-reloading cycles in the laboratory. By decomposing the total measured strains into reversible elastic and irreversible plastic components, this study quantitatively evaluates the evolution of plastic swelling and hardening mechanisms. The findings aim to understand how the stress history induced by excavation affects the mechanical behaviour, with a particular focus on plastic behaviour.

2 Experimental investigations

2.1 Material and testing device

The MHM URL is located in the Callovo-Oxfordian formation at a depth of approximately 490 m. At this level, a vertical and minor horizontal stress of about12.7 MPa, a major horizontal stress of 16 MPa, and a pore pressure of 4.5 MPa was reported from in-situ experiments (Wileveau et al. 2007). Previous characterisation of the COx claystone at this level reported an average water content of 7.9%, an average porosity of 17.5%, and a clay fraction of about 42% (Conil et al. 2018).

The core used in this study was extracted after the in-situ heating experiment named as CRQ(Plúa et al. 2024), which aims to better understand the thermally-induced hydro-fracturing of the COx claystone. A thermal loading and a corresponding thermal induced pore pressure were applied on the COx to generate tensile stresses higher than the tensile strength. For the core CRQ1733_03 used in this study, it was heated up to 95 °C for 1 month. After cooling down, the core was extracted and embedded in the T1 cell to minimize the mechanical degradation and damage due to the desaturation and microcracking (Ewy 2015; Conil et al. 2018).

Upon opening the packages in laboratory, the cores were immediately wrapped in tape to minimize moisture exchange with the atmosphere. The specimens were cored perpendicular to the bedding planes and machined to a disk with a diameter of 38 mm and a height of approximately 10 mm. Petrophysical characterization was performed using the remaining material. A bulk density of 2.41 g/cm^{3}was determined by hydrostatic weighing in a hydrocarbon, while the dry mass was obtained after oven-drying at 105 °C. Using a solid density of 2.72 g/cm^3 provided by Andra (Gaucher et al. 2004), a water content of 6.8%, a porosity of 17.5% and a degree of saturation of 92.7%were calculated. Additionally, a suction of 24.7 MPa was measured using a chilled-mirror dewpoint tensiometer. These results confirmed high degree of saturation of the specimen, indicating a good conservation of the moisture before laboratory testing. For long-term preservation, the specimen was wrapped in parafilm and aluminium foil and sealed in vacuum bags.

The experiment was performed using a temperature-controlled high-pressure isotropic compression cell (Mohajerani et al. 2012; Belmokhtar et al. 2017; Braun et al. 2021). The apparatus enables independent regulation of confining pressure, pore pressure, and temperature applied on the specimen. Confining pressure and pore pressure were controlled through two pressure–volume controllers. Thermal conditions were regulated by an external heating system surrounding the cell. Axial and radial strains were monitored by strain gauges attached on the specimen, with a reference gauge installed inside the cell to compensate for self-deformation and thermal drift.

2.2 Specimen preparation and loading procedure

The preparation and resaturation protocolis based on the methodology described in Braun et al. (2021) and are presented in Fig. 1a. After mounting, the drainage system was vacuumed to remove entrapped air. The specimen was then brought to an isotropic confinement pressure σ_{conf}=10 MPa and T = 25°C. Upon stabilization, synthetic pore water reproducing the in-situ chemical environment was injected into the specimen. Both σ_{conf} and pore pressure p_f were then increased at the same rate to remain an effective confining pressure σ'_{conf}= σ_{conf}-p_f of 10 MPa, with p_f=3.5 MPa. This resaturation phase, conducted under stress conditions representative of the in-situ state, lasted about ten days until the stabilization of measured swelling strains.

The experimental program on the resaturated specimen followed a multi-step loading procedure where each step comprised two successive phases. In the first phase, a rapid mechanical loading with a rate of ±100 kPa/min was applied. Given the very low permeability of the COx claystone, this rapid loading can be considered under pseudo-undrained, inducing transient pore pressure variation (Braun et al. 2018). In the second phase, the pore pressure inside the specimen returned to its prescribed value through a transient dissipation period. The stabilization of strains indicated hydraulic equilibrium, corresponding to the drained state. This study focuses exclusively on the drained behaviour. This step-by-step technique was utilized within a carefully designed cyclic loading framework to facilitate the analysis of material response. By comparing strain values obtained at identical stress levels during unloading-reloading cycles, the increments and accumulation of plastic strains could be decomposed from the total value and accurately evaluated.

Following this methodology, the test was conducted to investigate the mechanical behaviour after the in-situ thermal cycle and the potential effect raised from the excavation. The loading procedure was conducted through 36 steps and divided into three segments (Fig. 1b): The specimen was first unloaded from the initial stress state (σ'_{conf} =10 MPa) to σ'_{conf} =6 MPa and then reloaded to observe the initial expansion behavior (steps 1-7). This cycle was designed to mimic the stress release during the excavation (Conil et al. 2018). Following the unloading cycle, a loading-unloading cycle (steps 8-23) between 10 and 18 MPa was conducted to investigate the potential effect of previous unloading on the material behaviour during compression. A final cycle was performed between 6 MPa and 14 MPa to investigate the potential influence of the previous stress history on the subsequent development of irreversible strains, as further discussed in Section 3.

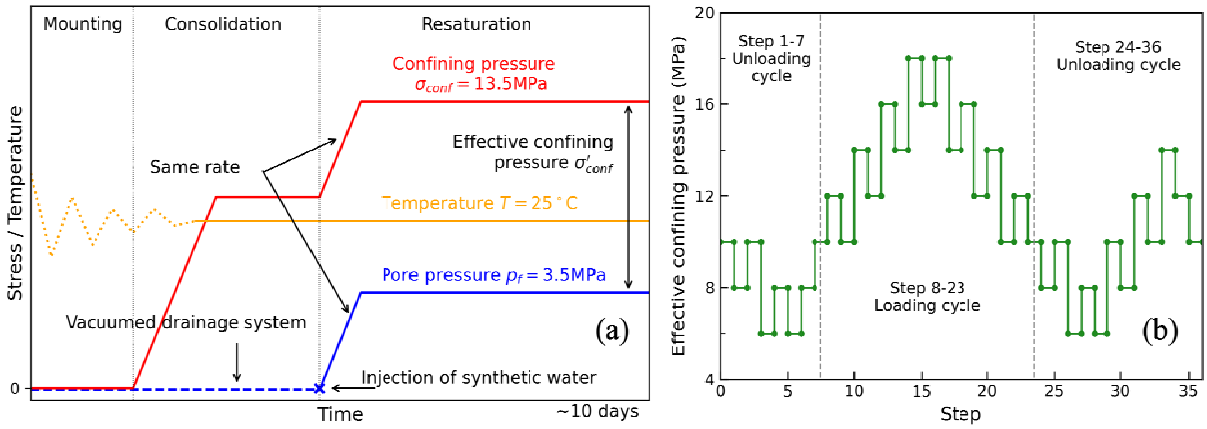


Fig. 1 Preparatory procedures (a) and the cyclic loading programme (b) applied in the isotropic test.(a) Evolution of confining pressure, temperature and pore pressure during mounting, consolidation and resaturation. Synthetic water was injected into the vacuumed drainage conduits after stabilization of confining pressure and temperature, leading to resaturation close to in-situ conditions. (b): Cyclic effective confining pressure applied during the test. The programme consists of three stages: an unloading cycle from 10 to 6 MPa (Steps 1–7), a loading cycle from 10 to 18 MPa (Steps 8–23), and a final cycle between6and 14 MPa (Steps 24–36).

3 Experimental results

The isotropic test was designed to reproduce the stress release and to investigate its impact on the mechanical behaviour of COx claystone. The measured strain under cyclic loading procedure is decomposed into the elastic (reversible) and plastic (irreversible) component, as shown in Fig. 2. The increment of plastic strain is evaluated by comparing the strain value difference, which is the result of the plastic behaviour between two steps. For example, following the path *abcd*, by comparing the states *a* and *d* we can identify the amount of irreversible axial plastic expansion which occurred during the unloading from 8 to 6 MPa.

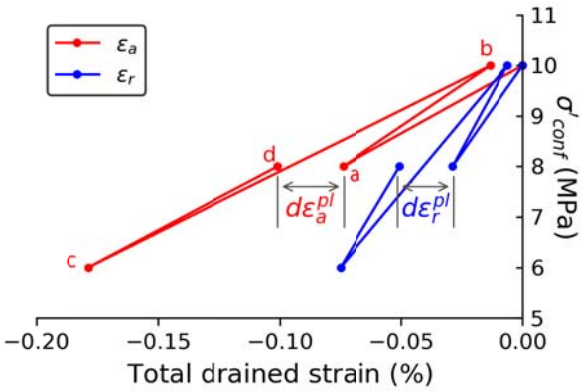


Fig. 2 Schematic diagram of strain analysis. Plastic strain increments $d\varepsilon^{pl}$ are evaluated by comparing total strain at the same stress level. For a given stress-strain path *abcd*, segments *ab* and *cd* are elastic, the strain difference between points *a* and *d* represents the plastic strain increment.

3.1 First unloading cycle: Swelling yield limit

The evolution of total drained strains and the decomposed plastic strains for the first cycle (Steps 1 to 7) are illustrated in Fig. 3a and Fig. 3b, respectively. During the initial unloading from σ'_{conf}= 10 MPa to 8 MPa, the specimen exhibits slight irreversible expansion in both axial and radial directions. This plastic swelling accumulates progressively as the effective confining pressure decreases. At the stress level of 6 MPa, the accumulated plastic strain reaches approximately 0.04% axially and 0.03% radially, accounting for approximately 30% of corresponding total drained strain. Such behavior indicates the activation of swelling yield mechanism at low confining pressure, which triggered the plastic expansion during the applied unloading path.

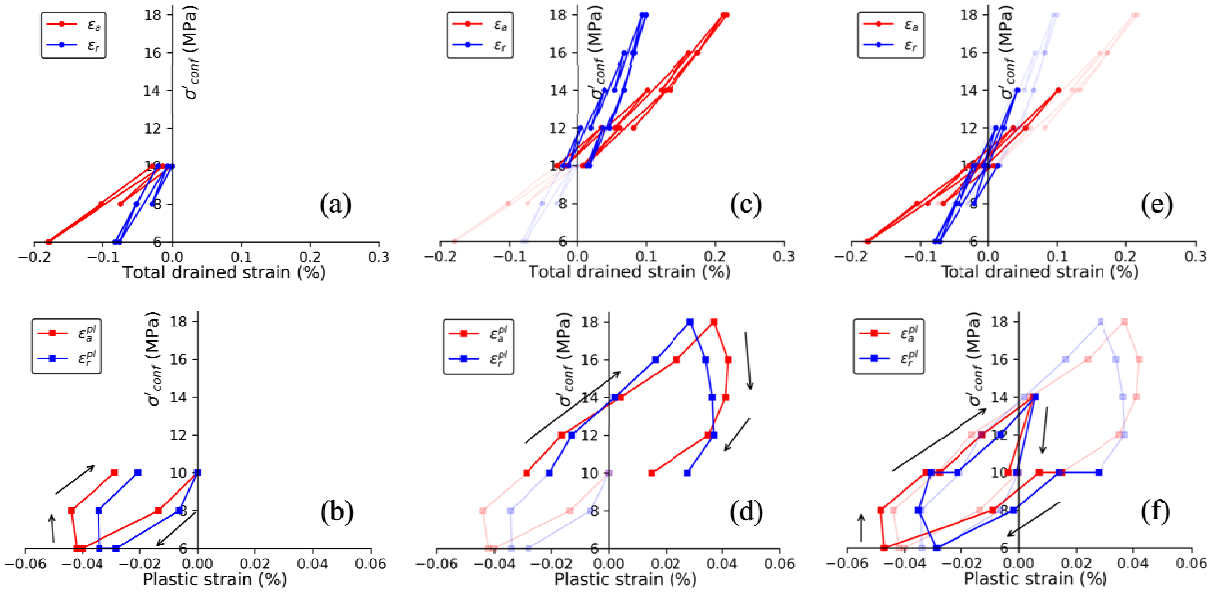


Fig. 3 Evolution of drained strains and corresponding plastic strains. Axial and radial drained strains of each loading or unloading step are shown in subplots (a), (c) and (e), while the corresponding decomposed plastic strains are shown in (b), (d) and (f). Arrows indicate the evolution of plastic strain. (a,b) First unloading cycle between 10 and 6 MPa. (c,d) Second loading cycle between 10 and 18 MPa. (e,f) An additional unloading cycle between 6 and 14 MPa.

During the subsequent reloading phase, the material response is mainly elastic between 6 and 8 MPa, with no significant variation in plastic strain. However, as σ'_{conf} increases above 8 MPa, a plastic

compression in both directions is observed. It is worth noting that this plastic compression initiated at 8 MPa, which is lower than the initial resaturated stress level of 10 MPa. This observation indicates that the previous unloading-induced plastic swelling led to a reduction in the compression yield limit, implying an interaction between the swelling and compression yield limits.

3.2 Second cycle: Compression-induced hardening of swelling yield limit

To further investigate the effect of stress history on the plastic response, a loading-unloading cycle was performed between 10 and 18 MPa (Steps 8 to 23), as shown in Fig. 3c and in Fig. 3d. During the cyclic loading steps, plastic compressive strains develop progressively, reaching approximately 0.037% in axial direction and 0.028% in radial direction. In the subsequent unloading phase, a predominantly elastic response is observed between 18 and 14 MPa, where plastic strains remain relatively stable. However, clear plastic expansion begins to develop in both directions once the effective confining pressure decreases below 12-14 MPa. This variation of the swelling yield limit, compared to the first unloading cycle, indicates an increase in this limit as a result of the previous plastic compression. This observation further implies the 1hardening effect of the compressive loading history on the swelling yield limit.

3.3 Final cycle: Validation of the coupled plastic compression-swelling response

An additional unloading-reloading cycle was conducted between 6 and 14 MPa (Steps 24 to 36) to verify the mutual influence and hardening effect between the two yield limits, as presented in Fig. 3e and Fig. 3f. During unloading from 10 to 6 MPa, plastic swellings continue to develop and reached similar values as the first unloading cycle when σ'_{conf}=6 MPa. During the subsequent reloading, an elastic response was again observed in 6 and 8 MPa, followed by the onset of plastic compression above this stress level. The plastic strains obtained during unloading from 14 to 10MPa show a small expansion in both directions, which can be interpreted as the material being within its elastic range or undergoing a small amount of plastic expansion.

4 Discussion

The mechanical response of the heat-treated COx claystone is governed by its loading history. The strain evolution and plastic behaviour reveal a stress-path dependency, where the yield limits for plastic swelling/compression mechanisms vary according to the stress history. Specifically, the consistent activation of plastic swelling during unloading phases confirms the existence of a swelling yield limit at low confinement. Conversely, subsequent reloading induces plastic compression, which can initiate at stress levels lower than the initial state depending on the previous expansion. These findings also suggest a narrow elastic domain bounded by two yield limits. Furthermore, the interaction between these limits indicates a coupling effect, where the activation of the compression mechanism leads to a hardening and shift of the swelling yield limit.

Such behaviour has been less discussed for COx claystone, but similar responses have been reported in other clayey materials. For instance, Cui et al.(2013), identified the bi-linear unloading/reloading paths in YP Clay, which were interpreted as transitions between mechanical-dominant and physico-chemical-dominant mechanisms. Additionally, loading-unloading cycles applied on Boom clay exhibited stress-strain hysteresis loops attributed to the high clay content (Yu et al. 2021). The plastic swelling phenomenon in such materials can be linked to the increase in the thickness of the adsorbed water layers. Given that the COx claystone in this study has a high clay content of 42%, a similar physico-chemical mechanism is likely responsible for the plastic swelling, and the stress-strain loops observed.

5 Conclusion

To investigate the effect of mechanical unloading on the mechanical response of the Callovo-Oxfordian claystone, a multistep isotropic unloading–reloading test was conducted on a specimen extracted after an in-situ heating experiment. By decomposing total strains into elastic (reversible) and plastic (irreversible) components, the following conclusions can be drawn:

1. During the unloading phase from the initial in-situ stress state, the specimen exhibits significant plastic swelling, suggesting the presence of a swelling yield limit at low confining pressure.

2. The plastic compression and swelling yield mechanisms exhibit a coupled behaviour. Plastic swelling during unloading reduces the compression yield limit, while subsequent compressive loading increases the swelling yield limit, demonstrating a mutual hardening effect controlled by stress history.

These results highlight the path dependency of the mechanical response of COx claystone. The excavation-induced stress release may alter the elastic domain and yield limits of the material prior to laboratory testing. Therefore, the effects of unloading during sampling and excavation should be considered when evaluating the THM performance of COx claystone. Future research focusing on microstructural evidence and advanced constitutive modelling will be useful to quantify these coupled hardening mechanisms.

References

Belmokhtar M, Delage P, Ghabezloo S, et al (2017) Poroelasticity of the Callovo–Oxfordian Claystone. Rock Mech Rock Eng 50:871–889. https://doi.org/10.1007/s00603-016-1137-3

Braun P, Ghabezloo S, Delage P, et al (2021) Transversely Isotropic Poroelastic Behaviour of the Callovo-Oxfordian Claystone: A Set of Stress-Dependent Parameters. Rock Mech Rock Eng 54:377–396. https://doi.org/10.1007/s00603-020-02268-z

Braun P, Ghabezloo S, Delage P, et al (2018) Theoretical Analysis of Pore Pressure Diffusion in Some Basic Rock Mechanics Experiments. Rock Mech Rock Eng 51:1361–1378. https://doi.org/10.1007/s00603-018-1410-8

Bumbieler F, Plúa C, Tourchi S, et al (2021) Feasibility of constructing a full-scale radioactive high-level waste disposal cell and characterization of its thermo-hydro-mechanical behavior. International Journal of Rock Mechanics and Mining Sciences 137:104555. https://doi.org/10.1016/j.ijrmms.2020.104555

Conil N, Talandier J, Djizanne H, et al (2018) How rock samples can be representative of in situ condition: A case study of Callovo-Oxfordian claystones. Journal of Rock Mechanics and Geotechnical Engineering 10:613–623. https://doi.org/10.1016/j.jrmge.2018.02.004

Corkum AG, Martin CD (2007) The mechanical behaviour of weak mudstone (Opalinus Clay) at low stresses. International Journal of Rock Mechanics and Mining Sciences 44:196–209. https://doi.org/10.1016/j.ijrmms.2006.06.004

Cui YJ, Nguyen XP, Tang AM, Li XL (2013) An insight into the unloading/reloading loops on the compression curve of natural stiff clays. Applied Clay Science 83–84:343–348. https://doi.org/10.1016/j.clay.2013.08.003

Ewy RT (2015) Shale/claystone response to air and liquid exposure, and implications for handling, sampling and testing. International Journal of Rock Mechanics and Mining Sciences 80:388–401. https://doi.org/10.1016/j.ijrmms.2015.10.009

Gaucher E, Robelin C, Matray JM, et al (2004) ANDRA underground research laboratory: interpretation of the mineralogical and geochemical data acquired in the Callovian–Oxfordian formation by investigative drilling. Physics and Chemistry of the Earth, Parts A/B/C 29:55–77. https://doi.org/10.1016/j.pce.2003.11.006

Mohajerani M, Delage P, Sulem J, et al (2012) A laboratory investigation of thermally induced pore pressures in the Callovo-Oxfordian claystone. International Journal of Rock Mechanics and Mining Sciences 52:112–121. https://doi.org/10.1016/j.ijrmms.2012.02.012

Plúa C, Vu MN, de La Vaissière R, Armand G (2024) In Situ Thermal Hydrofracturing Behavior of the Callovo-Oxfordian Claystone within the Context of the Deep Geological Disposal of Radioactive Waste in France. Rock Mech Rock Eng 57:4265–4283. https://doi.org/10.1007/s00603-023-03618-3

Wileveau Y, Cornet FH, Desroches J, Blumling P (2007) Complete in situ stress determination in an argillite sedimentary formation. Physics and Chemistry of the Earth, Parts A/B/C 32:866–878. https://doi.org/10.1016/j.pce.2006.03.018

Yu H, Chen W, Gong Z, et al (2021) Loading-unloading behavior of a clayey rock under thermo-hydro-mechanical conditions. International Journal of Rock Mechanics and Mining Sciences 148:104966. https://doi.org/10.1016/j.ijrmms.2021.104966

Zhang C-L, Armand G, Conil N, Laurich B (2019) Investigation on anisotropy of mechanical properties of Callovo-Oxfordian claystone. Engineering Geology 251:128–145. https://doi.org/10.1016/j.enggeo.2019.02.008